THE ASTROPHYSICAL JOURNAL, 346:251–264, 1989 November 1

A COMPACT PLANETARY NEBULA AROUND THE HOT WHITE DWARF EGB 6/PG 0950+139[1]

JAMES LIEBERT,[2,3,4] RICHARD GREEN,[5] HOWARD E. BOND,[6] J. B. HOLBERG,[3,7] F. WESEMAEL,[3,8]
THOMAS A. FLEMING,[2] AND KENNETH KIDDER[7]

Received 1989 February 1; accepted 1989 April 28

ABSTRACT

EGB 6 is a very large (11′ × 13′) planetary nebula of low surface brightness whose central star (0950+139) is a very hot DA/DAO white dwarf. However, the nucleus also shows strong emission lines of [O III], [Ne III], hydrogen, and helium, which do not arise in the old, faint shell but instead are confined to an unresolved nebular core component of apparently newly ejected matter.

Fitting of the wings of the broad Hγ absorption line in the stellar spectrum yields $T_{\rm eff} = 70{,}000 \pm 7000$ K, $\log g = 7.5 \pm 0.25$, and establishes that hydrogen is the dominant element in the atmosphere. These parameters place the central star near the hot extreme of the known sequence of DA (DAO) white dwarfs. Helium absorption lines appear to be present, but the helium abundance in the photosphere is difficult to determine because of the masking by emission lines.

Analysis of the line spectrum of the unresolved central nebula indicates a very high density ($4 \times 10^5 < N_e < 10^7$ cm^{-3}), and a very small ionized nebular mass between 3×10^{-10} and $7 \times 10^{-8}\ M_\odot$, with a physical extent of order 10 AU. An observed limit on the nebular expansion rate (≤ 50 km s^{-1}) leads to a crossing time of the order of a year (unless the filling factor is much less than unity). There is no evidence for variation in the emission-line fluxes over 9 yr. The oxygen and neon abundances appear to be normal for Galactic disk gas, while helium may be modestly enriched.

Three kinds of scenarios are discussed to account for the existence of this peculiar nebula, but none appears terribly promising. The first possibility considered is that the nebula was ejected from the white dwarf as a discrete event; this hypothesis is heavily constrained by the nebular size, density, and expansion rate, by the low luminosity and radius of the star, and by the absence of evidence for variation in density-sensitive forbidden lines from 1978 to 1987. On the other hand, we are aware of no plausible mechanism to cause the observed amount of mass to be lost directly from a white dwarf in a steady or sporadic wind, at outflow velocities orders of magnitude below the escape velocity. Finally we consider the possibility that the gas is lost from a close companion star, but we find no evidence that this is a close binary system.

Subject headings: nebulae: abundances — nebulae: individual (EGB 6) — nebulae: planetary — stars: white dwarfs — ultraviolet: spectra

I. INTRODUCTION

Analyses of the photospheres of planetary nebula nuclei (PNNs) have revealed a few highly evolved objects that have nearly reached their final white dwarf radii. For example, the nucleus of Abell 7 (Mendez *et al.* 1981; Wesemael, Green, and Liebert 1985) is a white dwarf with a hydrogen-rich atmosphere (type DAO). Moreover, a search for residual nebulosity around hot degenerate stars revealed evidence for a faint nebula around PG 0108+101 (Reynolds 1987), a helium-rich white dwarf of type DO. Both nebulae are very extended (>20′ diameters) and of low surface brightness. To be sure, it is difficult to establish whether the latter is a residual planetary nebula (PN) or just ambient, ionized gas. However, there appears to be a general tendency for large "old" nebulae of low surface brightness to be associated with PNNs of higher surface gravity, which are farther along their evolutionary tracks to the white dwarf stage.

In this paper we will discuss the remarkable central star of the planetary nebula EGB 6. The nebula was discovered by H. E. B. in 1978 during an examination of Palomar Sky Survey prints and was included in a list of new planetary nebulae of low surface brightness published by Ellis, Grayson, and Bond (1984, hereafter EGB). On the Sky Survey prints, EGB 6 appears as an extremely faint, nearly circular rim whose dimensions are 11′ × 13′.

The central star was identified by H. E. B. on the basis of its extremely blue color on the Palomar prints, and a finding chart is given in EGB. Spectroscopic observations of the nucleus were obtained in 1978 with the KPNO 2.1 m telescope and intensified image dissector scanner (IIDS). In addition to a broad Hγ absorption line, the spectrum (Fig. 1) shows strong emission lines, including forbidden lines of [O III] and [Ne III]. Because of the extremely low surface brightness of the nebular

[1] Some observations were obtained at the Multiple Mirror Telescope Observatory, jointly operated by the Smithsonian Center for Astrophysics and the University of Arizona. Other ground-based observations were obtained at Palomar Observatory, a facility of the California Institute of Technology, at the Kitt Peak National Observatory, and at the Steward Observatory.

[2] Steward Observatory, University of Arizona.

[3] The Observatories of the Carnegie Institution of Washington.

[4] Guest Observer at the *International Ultraviolet Explorer* (*IUE*) Observatory, operated by the NASA/Goddard Space Flight Center, Greenbelt, Maryland.

[5] Kitt Peak National Observatory, National Optical Astronomy Observatories, operated by the Association of Universities for Research in Astronomy (AURA), Inc., under contract with the National Science Foundation.

[6] The Space Telescope Science Institute, Baltimore, Maryland, operated by AURA under contract to NASA.

[7] Lunar and Planetary Laboratory, University of Arizona.

[8] Département de Physique, Université de Montréal.

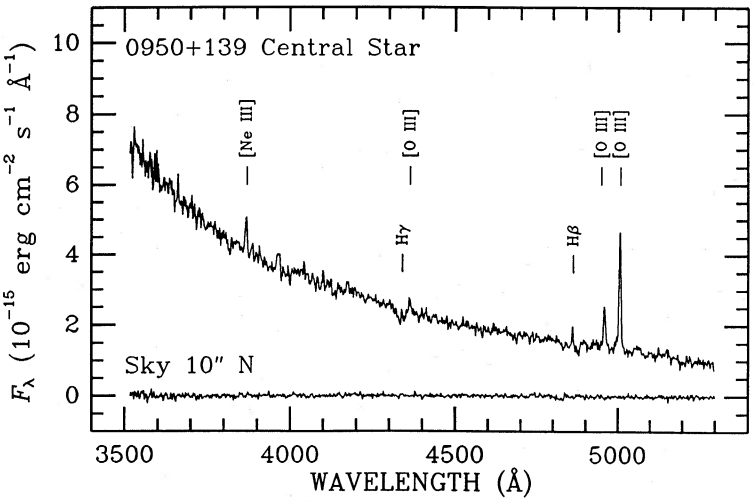

FIG. 1.—IIDS spectrum of the 0950+139 central star and associated nebular component and of a patch of sky 10″ north of the star, obtained in 1978. The emission lines are completely absent in the latter, which indicates that the nebular component centered on the star is distinct from the much fainter, extended shell visible on the Palomar Sky Survey prints.

image and its apparent confinement to a rim several arcminutes away from the nucleus, it was quite surprising to detect strong emission lines in the spectrum (taken with an entrance aperture having 4″ diameter) centered on the PNN. Hence, a second observation was taken of the sky 10″ north of the star (also shown in Fig. 1). No emission lines were detected, thus confirming that the nebula includes a separate, bright core component.

The nucleus was also independently discovered in the Palomar Green (PG) Survey (Green, Schmidt, and Liebert 1986), and was designated PG 0950+139. The photographic *B*-magnitude obtained in the 1973–1974 time frame was 15.7. A SIT Vidicon classification spectrum obtained with the Palomar 5 m telescope in 1979 also showed the strong nebular spectrum; moreover, the nebular component appeared to be confined to the stellar seeing image on the two-dimensional SIT frame. In a subsequent analysis of higher resolution spectrophotometry, the PNN was placed in the highest temperature category of DA white dwarfs (Fleming, Liebert, and Green 1986).

In § II of this paper, we present a variety of follow-up observations which are relevant to the analyses of both the nebula and the stellar photosphere. A more detailed analysis of the central star's photosphere, based primarily on the optical line spectrum, is presented in § III. The analysis of the emission-line spectrum and the derivation of the nebular parameters are given in § IV. We consider three scenarios to explain the existence of this unusual nebula in § V. A preliminary presentation of some of these results was given by Liebert (1989). In addition, it should be noted that a second paper has been written in which a detailed photoionization model of the nebula is presented and a different model to explain the object is developed (Dopita and Liebert 1989).

II. SPECTROPHOTOMETRY AND PHOTOMETRY

a) Optical Spectra

Ten spectroscopic observations have been obtained during the period 1978–1987. Table 1 is a log of the relevant information. The first two observations were discussed in § I. Four spectra at 2 Å resolution were obtained with the Steward Observatory (SO) 2.3 m reflector, Cassegrain spectrograph, and intensified, photon-counting Reticon (PCR). The two best blue PCR spectra (obtained in 1987 February) were used in the photospheric absorption-line fit and are displayed in Figure 2. The model atmospheres analysis is discussed in § III*a*. A PCR spectrum covering the optical ultraviolet was obtained in 1985 and is useful in placing limits on the important [Ne V] and [O II] forbidden lines. Equivalent widths (EWs) measured for these emission lines are listed in Table 2A and some absolute line fluxes are given in Table 2B. Sources of error and crude error estimates are discussed in § IV.

Two complementary observations at red wavelengths were obtained with the KPNO 4 m telescope and cryogenic camera using an 800 × 800 Texas Instruments CCD detector. However, these data have a much lower resolution of 15 Å. The strong emission lines of [O III] and Hα are noteworthy in these CCD spectra, as shown in Figure 3. Equivalent widths are listed in Table 2A and absolute line fluxes in Table 2B. In addition, these two-dimensional spectra permit quantitative limits on the spatial extent of the inner nebula along the direction of the slit (§ IV*c*).

More accurate spectrophotometry of the 3300–9000 Å region is provided by an observation with the Palomar 200 inch (5 m) telescope and multichannel spectrophotometer (MCSP; Oke 1974); these data are discussed in the following subsection and included in Figure 4. Finally, high resolution

TABLE 1

LOG OF SPECTROSCOPIC OBSERVATIONS

Date	Telescope/System	Wavelength Range (Å)	Resolution (Å)
1978 Apr 11	KPNO 2.1 m IIDS	3500–5400	7
1979 Feb 26	Palomar 5 m SIT	4000–6600	15
1980 Dec 27	Palomar 5 m MCSP	3200–9000	80, 160[a]
1985 Feb 19	KPNO 4 m CCD	4400–7500	15
1985 Apr	SO 2.3 m Reticon	3850–5000	2
	SO 2.3 m Reticon	3200–4000	2
1987 Apr 25	*IUE* SWP 40572 low	1200–2000	7
1987 Feb 1	SO 2.3 m Reticon	3900–5000	2
1987 Feb 2	SO 2.3 m Reticon	3900–5000	2
1987 Mar 1	KPNO 4 m CCD	4400–7500	15

[a] Resolution 80 Å for 3200–5700 Å, 160 Å at longer wavelengths.

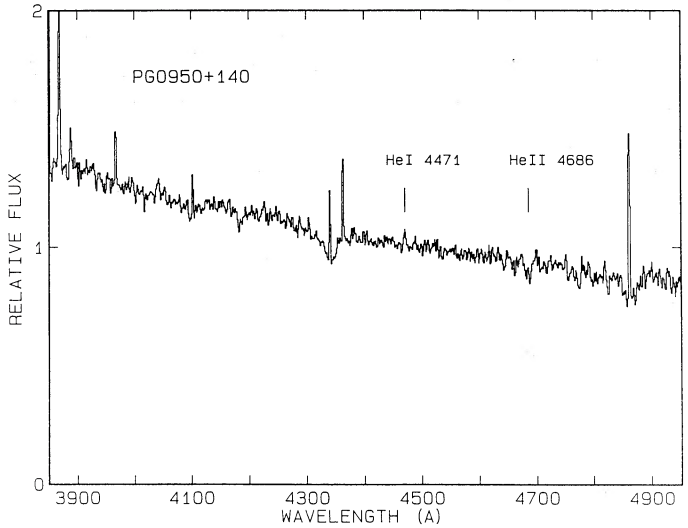

FIG. 2.—Summed Steward Observatory 2.3 m Reticon spectra at blue wavelengths with 2 Å spectral resolution. The broad H and probable He II 4686 Å absorption lines are indicative of a DAO white dwarf (§ III*a*). Prominent emission lines include [Ne III] λ3869, [O III] λ4363, and the Balmer lines Hβ through Hε. He I 4471 Å and probable He II 4686 Å emission are also seen.

measurements of the emission lines He II λ4686 and Hα were obtained with the MMT echelle spectrograph, primarily for the purpose of estimating the expansion velocity of the compact nebula (§ IV*e*). These are shown in Figure 5.

b) Ultraviolet Spectrophotometry

An ultraviolet spectrum of the central star was obtained with the *International Ultraviolet Explorer* (*IUE*) satellite on 1987 April 25. The 100 minute exposure with the SWP camera covered the 1175–1975 Å wavelength range; the low-dispersion mode afforded a spectral resolution of 7 Å. The large (10″ × 20″) aperture would have included only an insignificant portion of the surrounding large, faint nebula, but all of the compact component. In fact, only the very bright stellar continuum is clearly detected in the spectrum, displayed here as Figure 6. No photospheric absorption features of He II 1640 Å or resonance metal lines are identifiable, and no plausible nebular lines are detected at their expected wavelengths. The coarse spectral resolution and small telescope aperture make it particularly difficult for any narrow nebular emission lines to compete against the stellar component, which has a sharply rising Rayleigh-Jeans slope in the ultraviolet. A reasonable estimate of an upper limit to any emission-line intensities would be 5×10^{-14} ergs cm^{-2} s^{-1}. The geocoronal Lyα would effectively cover both the nebular emission and the photospheric absorption due to that transition. Comparison with Figure 2 suggests that He II 1640 Å nebular emission and photospheric absorption components may effectively cancel out at this lower resolution. In fact, the *IUE* spectrum of the nucleus of Abell 7, a star of similar temperature and gravity, also shows no convincing stellar absorption or nebular emission lines (Wesemael, Green, and Liebert 1985).

c) Optical Photometry

Two photometric observations of the central star on the *UBV* system have been obtained, and results are given in Table 3. Both were obtained with the KPNO No. 2 0.9 m telescope, the first by H. E. B. and A. D. Grauer and the second by Grauer (as quoted by EGB). Because of the faintness of the star and the small number of standard-star observations, the magnitude and colors are accurate only to ±0.05 mag; thus there is no indicated gross variability of the star over a 4 yr interval bracketing the time of the MCSP scan.

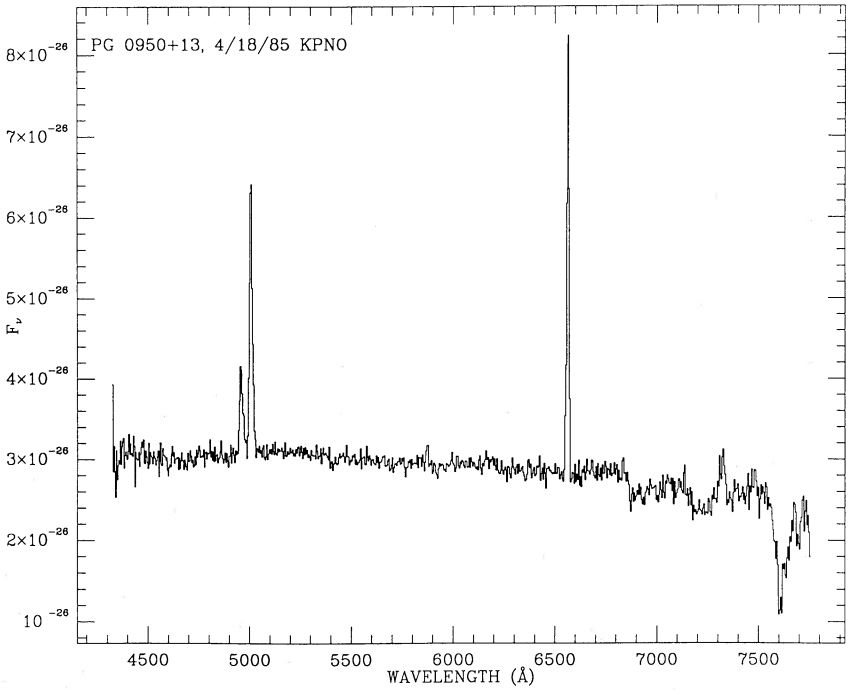

FIG. 3.—Red KPNO 4 m cryocam CCD spectrum showing the nebular spectrum atop the very blue stellar continuum. The lower spectral resolution (15 Å) leads to a nearly complete cancellation of the Hβ and He II 4686 Å emission and photospheric absorption, in comparison with the spectrum in Fig. 2.

TABLE 2A

EQUIVALENT WIDTHS FOR EMISSION LINES (Å)

Line (1)	Wavelength (Å) (2)	1978 5 m SIT (3)	1978 2.1 m IIDS (4)	1985 4 m CCD (5)	1985 2.3 m PCR (6)	1985 2.3 m PCR (7)	1987 4 m CCD (8)	1987 2.3 m PCR (9)
[Ne v]	3425	...	...	...	...	< 0.3	...	...
[O II]	3727[a]	...	...	...	...	<0.2	...	...
[Ne III]	3869	...	1.6	...	1.7	1.6	...	2.0
[S II]	4069[a]	...	...	...	<0.2	...	...	...
Hδ	4101[b]	...	...	...	0.2:	...	...	0.4
Hγ	4340[b]	...	1.0	...	0.9	...	...	0.9
[O III]	4363[a]	...	1.1	...	1.4	...	...	1.0
He I	4471	...	...	...	0.2:	...	...	...
He II	4686[b]	...	...	...	0.2:	...	...	...
[Ar IV]	4712[c]	...	...	...	0.5	...	...	...
[Ar IV]	4740	...	...	...	0.2:	...	...	...
Hβ	4861	...	3.0:	...	2.9	...	...	2.8
[O III]	4959[a]	4:	5.6	6.0	5.1	...	5.0	...
[O III]	5007[a]	15:	17.2	18.3	18.5	...	17.9	...
He I	5876	...	...	0.9	...	...	...	...
[O I]	6300	...	...	1.5	...	...	...	...
Hα	6563	19:	...	22.5	...	...	24.3	...
He I	6678	...	...	0.7	...	...	...	...
[S II]	6717, 6731[a]	...	...	<1	...	...	...	...
[O II]	7325	...	...	1.5:	...	...	...	...

[a] Measured equivalent width probably affected by density quenching.
[b] Measured equivalent width probably affected by photospheric absorption.
[c] Probably a blend with He I.

TABLE 2B

EMISSION-LINE FLUXES (10^{-14} ergs cm^{-2} s^{-1}) MEASURED FROM FLUX-CALIBRATED, SMALL-APERTURE SPECTRA

Line (1)	Wavelength (Å) (2)	1978 IIDS (3)	1985 CCD (4)	1987 CCD (5)	1987 2.3 m (6)
[Ne III]	3869	7.0			4.6
Hγ	4340[a]	2:			1:
[O III]	4363	2.5			1.4
Hβ	4861[a]	4:			2.4
[O III]	4959	8.5	12	10	
[O III]	5007	27.0	38	32	
Hα	6563		20	15	

[a] Measured flux may be affected by photospheric absorption.

TABLE 2C

MEAN LINE FLUXES (10^{-14} ergs cm^{-2} s^{-1})

Line	Wavelength	Adopted EW (Å)	Continuum Flux ($\times 10^{-15}$)	Line Flux
[Ne v]	3425	<0.3	8.36	<2.5
[O II]	3727[a]	<0.2	6.16	<1.2
[Ne III]	3869	1.7	5.37	9.1
[S II]	4076[a]	<0.2	4.44	<0.9
Hδ	4101[b]	0.4	4.34	1.7
Hγ	4340[b]	0.9	3.53	3.2
[O III]	4363[a]	1.1	3.47	3.8
He I	4471	0.2:	3.17	0.6:
He II	4686[b]	0.2:	2.67	0.5:
[Ar IV][c]	4712	0.5	2.62	1.3
[Ar IV]	4740	0.2:	2.56	0.5:
Hβ	4861[b]	2.9	2.34	6.8
[O III]	4959[a]	5.4	2.17	11.7
[O III]	5007[a]	17.9	2.10	37.5
He I	5876	0.9	1.17	1.1
[O I]	6300	1.5	0.91	1.4
Hα	6563	23.3	0.78	18.2
He I	6678	0.7:	0.73	0.5:
[S II]	6717, 6731[a]	<1	0.71	<0.7
[O II]	7325	1.5:	0.52	0.8:

[a] Measured flux probably affected by density quenching.
[b] Measured flux may be affected by photospheric absorption.
[c] Blend of [Ar IV] and He I.

Five hours of high-speed photometry obtained on two nights by Bond and Grauer (1987) likewise showed no evidence for short-term variability. This result provides evidence that the star is not an interacting binary with a significant amount of ongoing mass transfer, and that it is probably not a close, detached binary, as discussed in § Vc. The lack of observed photometric variations also suggests that 0950+139 is not a pulsating variable.

d) Spectral Energy Distribution

We have constructed an overall energy distribution for the central star in Figure 4, under the assumption that it is non-variable. Since the *IUE* spectrum showed only the continuum of the hot stellar component, we have binned the fluxes into 25 Å intervals. There is an apparent discrepancy between the monochromatic MCSP magnitudes near 5500 Å and the broad-band photometry of Table 3. Abbreviated MCSP colors listed in Green, Schmidt, and Liebert (1986) indicate $V = m(5500\ \text{Å}) = 16.37$. The V-magnitude from EGB is erroneously listed as "B" in this last reference. Since the MCSP observing was done with some clouds noted in the sky, we have

TABLE 3

UBV PHOTOMETRY OF 0950+139

UT Date	V	$B-V$	$U-B$
1978 Apr 10.....	16.05	−0.25	−1.19
1982 Apr 24.....	16.00	−0.34	−1.25

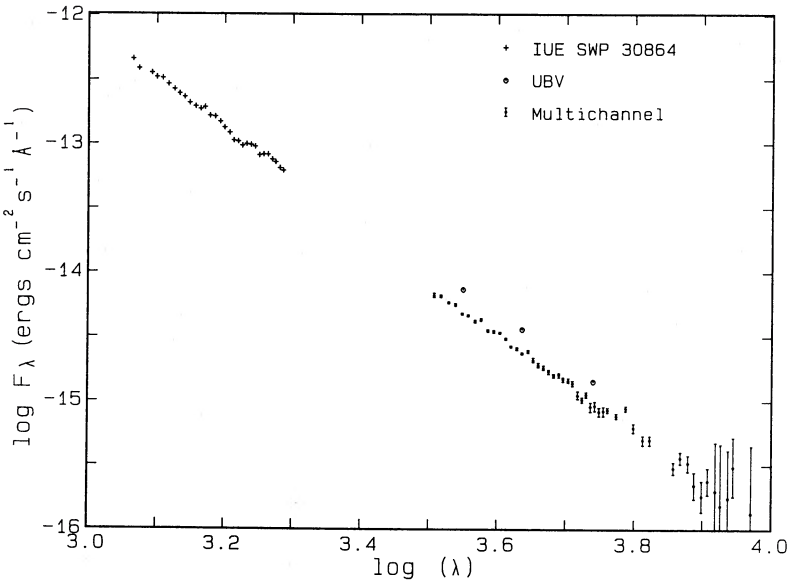

FIG. 4.—Absolute energy distribution of the 0950+139 nucleus, including ultraviolet *IUE* (*plus signs*), optical MCSP data (*filled circles with error bars*), and *UBV* photometric flux points (*open circles*). The MCSP data provide an accurate slope of the optical continuum but are uniformly fainter than the *UBV* flux points because of the presence of thin clouds.

also plotted the *UBV* broad-band points in Figure 4, and these fall some 0.4 mag brighter than the MCSP data set.

The *IUE* and *UBV* fluxes may fit well with a power law of slope −3.69. This is even slightly steeper than the slope of −3.59 for the hot DA white dwarf G191-B2B, for which Holberg, Wesemael, and Basile (1986) estimate $T_{\rm eff} = 62{,}250 \pm 3520$ K. G191-B2B may currently be the hottest well-analyzed DA star. Over the optical bandpass alone, the energy distribution normalized to the absolute values of the *UBV* flux points is well approximated by the power law

$$\log f_c = -3.65 \log \lambda - 1.175 , \qquad (1)$$

where f_c is assumed to be the continuum flux, since the nebular lines are weak. The very blue slope for the planetary nucleus suggests (1) that this star is as hot or hotter than G191-B2B and (2) that there is essentially no reddening in the line of sight, as expected for the high Galactic latitude of +46°. Since these data cover only the Rayleigh-Jeans tail of the energy distribution, we prefer the method discussed in the next section to derive a more accurate estimate of the effective temperature.

III. ATMOSPHERIC PARAMETERS OF THE CENTRAL STAR

a) Model Atmosphere Fits to the Photospheric Spectrum

The blue spectrum (see Fig. 2) includes an underlying photospheric component with broad hydrogen and probable He II and He I absorption lines. Superposed on this continuum are several nebular emission lines. The photospheric spectrum appears similar to those of hot DA and DAO white dwarfs

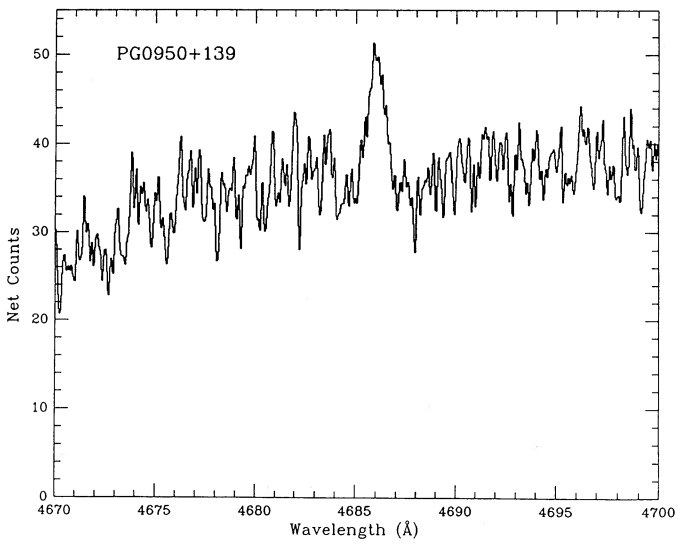

FIG. 5*a*

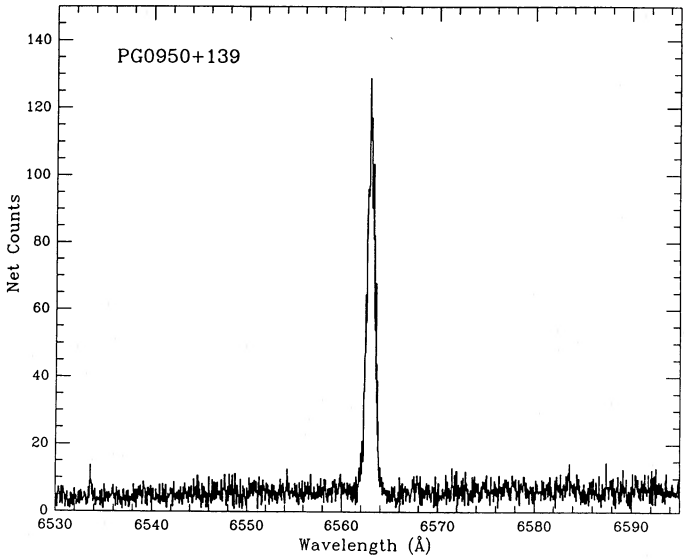

FIG. 5*b*

FIG. 5.—MMT echelle spectra covering (*a*) the He II 4686 Å emission line and (*b*) the Hα line

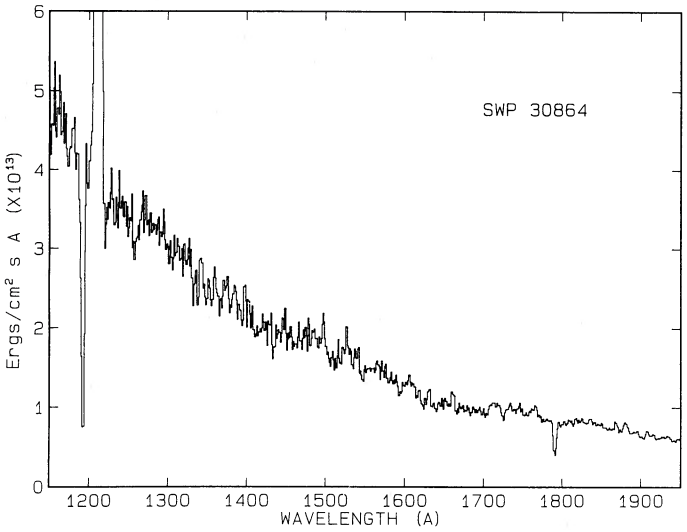

FIG. 6.—Short-wavelength *IUE* spectrum of 0950+139. The strong Lyα emission is probably geocoronal. A reseau point produces a spurious absorption feature near 1790 Å. No nebular emission lines are clearly detected.

displayed in Holberg (1987), for which atmospheric parameters are estimated in Holberg *et al.* (1989); however, the masking effect of the emission makes it difficult to assess the photospheric helium abundance, whose range spans at least 3 orders of magnitude in DA/DAO white dwarfs with $T_{\rm eff} \geq 50{,}000$ K or hotter (Petre, Shipman, and Canizares 1986; Paerels 1987; Vennes *et al.* 1988). In our analysis, we attempt to estimate the photospheric temperature and surface gravity from the uncontaminated absorption wings of the Balmer lines.

In analyzing the photospheric spectrum, we utilize calculations of models applicable to hot, high-gravity stars; characteristics of the model set, in which local thermodynamic equilibrium (LTE) is assumed, are described in essence in Wesemael *et al.* (1980). We have already noted that any weak photospheric helium features are hidden by the nebular spectrum. The DA/DAO spectrum indicates that the He/H abundance should be much smaller than unity. A trace value for the helium abundance has a minimal effect on the hydrogen-line profiles. It is therefore entirely appropriate to fit the best observed of the hydrogen lines, Hγ, with a series of pure hydrogen models, varying the two parameters $T_{\rm eff}$ and log g. The achievement of consistency with the Hβ, Hδ, and Hε equivalent widths was a secondary consideration. The technique is applied to several hot DA and DAO stars in Holberg *et al.* (1989).

In Figure 7 we show fits of a sequence of these models to the Hγ (4340 Å) absorption-line data for log $g = 7.5$ and a bracketing range of $T_{\rm eff}$ on a more expanded plot scale than that of Figure 2. The best fit for this set is from the model at $T_{\rm eff} =$ 70,000 K. Sequences with the same temperatures were also calculated at values of log $g = 8.0$ and 7.0. The former produced profiles which are systematically too broad. The latter sequence predicts profiles which are systematically weaker and narrower. At best a marginal fit in the range 60,000–65,000 K and log $g = 7.0$ is possible. In general, we believe that a 10% uncertainty (±7000 K) is appropriate for the temperature, and that log $g = 7.5 \pm 0.25$. These values are adopted in later calculations. Note that the evolutionary models of Koester and Schönberner (1986, hereafter KS) for 0.6 $M_\odot$ and surface hydrogen layer masses of 10^{-4} $M_\odot$ and zero predict log g values at $T_{\rm eff} = 70{,}000$ K near 7.7 and 7.8, respectively. An adopted mass of 0.6 $M_\odot$ is close to the means for white dwarfs and planetary nuclei (cf. Weidemann and Koester 1984; Schönberner 1986). The sample of hot DA and DAO white dwarfs analyzed in Holberg *et al.* (1989) have a mean log g near 7.5, so that 0950+139 does not appear to be abnormally high or low in mass. We doubt that the uncertainties in the LTE models and in the hydrogen line broadening are small enough to rule out this object fitting a KS model at log $g = 7.8$. The derived parameters therefore confirm that EGB/PG 0950+139 has already entered the white dwarf cooling track. The same models indicate a cooling age of a few times 10^5 yr, if the mass is not too different from 0.6 $M_\odot$.

b) Luminosity, Distance, and Limit on Reddening

The absolute bolometric magnitude of the star may be estimated from the derived $T_{\rm eff}$ and log g values, but a value of the radius (i.e., the mass) must be assumed. As previously noted, the derived log g is 0.2–0.3 smaller than predicted by the KS models appropriate to the mean white dwarf mass of 0.6 $M_\odot$ at $T_{\rm eff} = 70{,}000$ K, although the disagreement is of marginal significance. It is questionable how far one should push the application of (1) the empirical values and (2) the values of specific KS models. The implication of believing both is that the stellar mass is smaller than 0.6 $M_\odot$, since lower mass stars are expected to be larger and more luminous at a given temperature. In fact, the KS model for 0.546 $M_\odot$ and a thick (10^{-4} $M_\odot$) hydrogen layer fits the mean values of our derived stellar parameters. If the outer hydrogen-layer mass is much thinner

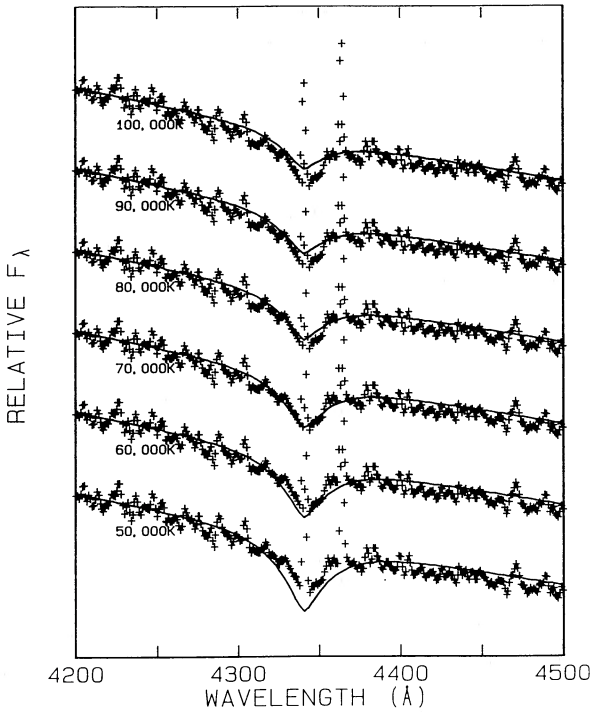

FIG. 7.—Sequence of model atmosphere fits to the photospheric Hγ line profile. The observed fluxes (*plus signs*) are a detailed plot from Fig. 2. The synthetic spectra (*smooth curves*) are from pure hydrogen models with log $g = 7.5$, assuming LTE, and $T_{\rm eff}$ ranging from 50,000 K to 100,000 K as labeled. The [O III] 4363 Å, the nebular Hγ, and He I 4471 Å emission lines are seen as upward "spikes," although several wiggles evident at this scale in the data are attributable to Reticon pattern noise.

than this (which we argue later is more plausible), then the implied mass would be smaller still, perhaps 0.5 $M_\odot$.

We now consider two cases in which the mass of 0950+139 is assumed to be $M_1 = 0.6\ M_\odot$ and $M_2 = 0.5\ M_\odot$. From the previous determination of $\log g = 7.5 \pm 0.25$, we obtain radii of $R_1 = 0.023(+0.008, -0.006)\ R_\odot$ and $R_2 = 0.021(+0.007, -0.005)\ R_\odot$. The corresponding luminosities, including a 10% uncertainty in $T_{\rm eff}$, are $\log L_1/L_\odot = 1.05 \pm 0.24$ and $\log L_2/L_\odot = 0.97 \pm 0.23$, or, alternatively, $(M_{\rm bol})_1 = +2.12 \pm 0.6$ and $(M_{\rm bol})_2 = +2.32 \pm 0.6$ (with some rounding of error bars).

Using R_1 and R_2 from above, $T_{\rm eff} = 70{,}000 \pm 7000$ K, and bolometric corrections from Wesemael *et al.* (1980), we estimate $(M_v)_1 = +7.75(+0.69, -0.58)$ and $(M_v)_2 = +7.64(+0.63, -0.59)$. The visual magnitudes are more sensitive to changes in the radius and mass than in the $T_{\rm eff}$, but the uncertainty in the M_v due to mass is modest and we can conclude that $M_v = +7.7 \pm 0.7$. Using the observed $V = 16.02$ then leads to a photometric distance estimate of 460(+174, −126) pc, which will be assumed subsequently.

The absence of any indication of a reddened ultraviolet slope (§ II*b*) may be stated more quantitatively as a limit on the ultraviolet extinction of $A_{1200\,\text{Å}} \leq 0.2$ mag, generously. This corresponds (Seaton 1979) to $E_{B-V} \leq 0.02$ in the line of sight to 0950+139. This last value corresponds very approximately to a limit on the column density of hydrogen (Spitzer 1978, p. 156) of $\leq 1.2 \times 10^{20}$ cm^{-2}. Generally, such small values might be inconsistent with a distance of several hundred parsecs, but 0950+139 lies at high Galactic latitude ($b = +46°$) some 330(+130, −90) pc above the plane. Inspection of the 21 cm maps of Heiles (1975) yields an estimate of $N_{\rm H} = 3.5 \times 10^{20}$ cm^{-2} in the direction of 0950+139, most of which should be confined to a scale height <200 pc and therefore in front of the star. Given the scatter of observations near the origin of various plots used to determine the $N_{\rm H}$ versus E_{B-V} relation, the modest limit on the hydrogen column density is not inconsistent with the distance estimate and range.

Finally, the results presented above would place 0950+139 about 1 disk scale height above the Galactic plane. The radial velocity measurements discussed in § IV are consistent with the conclusion that the star is most likely part of the disk population.

c) Limits on a Red Companion

The parameters derived here and the absence of an upturn at the red end of the energy distribution also allow constraints to be placed on the luminosity of any low-mass, main-sequence companion. If we make the conservative assumption that such a cool star does not contribute as much as half of the observed flux at 8000 Å, a value appropriate to an M dwarf at approximately absolute $M(8000) = +9.6$. This corresponds to the statement that any companion is not more luminous (earlier) than spectral type M3–M4 V.

IV. ANALYSIS OF THE EMISSION-LINE SPECTRUM

Because of the small entrance apertures used for most of the spectroscopic observations (§ II*a*), the most reliable way of combining and comparing measurements of emission-line strengths from this diverse data set is to present equivalent widths. The assumption implicit in this technique is that the continuous energy distribution of the central star does not vary and can be used to normalize the measured line fluxes and that the emission-line region is unresolved. We have presented evidence that the star is not a short-term photometric variable (§ II*c*). There is also no evidence that it has varied in mean brightness over the last 9 years, although some amount of long-term variation cannot be ruled out. The equivalent widths measured for all spectroscopic observations are listed in Table 2A.

In addition, we list absolute nebular emission-line fluxes in Table 2B as determined from the observations which we regard as having the best absolute and relative flux calibrations. These include the IIDS observation, which utilized a 4.″3 circular entrance aperture and provides a crucial test for gross changes over the 9 year baseline (§ IV*f*). Also shown are fluxes derived from the long-slit CCD spectra. Finally, we show the sum of two 1987 February PCR spectral, although these were obtained with smaller 3″ apertures, from which any spillover would result in reduced measurements of absolute fluxes. We thus would not believe flux differences of 50% among these measurements as indicating real variations, especially if corresponding differences in equivalent widths (Table 2A) are not observed.

It is standard in presenting planetary nebula line fluxes to give an absolute value for Hβ and normalize the measurements of other lines to a scale with Hβ equal to 100. We do not follow the convention, since our Hβ values are among the more uncertain measurements. In particular, the apparent emission-line strength is weakened by blending with the photospheric absorption line, and the amount of blending is particularly sensitive to the spectral resolution. For example, the emission and absorption components almost completely cancel out in the CCD spectra (Fig. 3). Conversely, the PCR spectra at 2 Å resolution provide the most accurate measurements of the Hβ emission-line flux. Given the case made below for quenching of some of the forbidden lines, we also do not choose to normalize to the strong, unambiguously measured [O III] lines. We also list absolute fluxes only for the strongest lines.

For the estimate of nebular parameters in this section, it is nonetheless necessary to derive the best estimates for the line fluxes for both strong and weak lines using the data sets obtained at different times, covering different wavelength ranges, at different spectral resolutions, and with differing absolute photometric accuracies. For this purpose, we rely on the equivalent widths listed in Table 2A and normalize these to the stellar energy distribution given by equation (1). Table 2C lists the adopted set of line fluxes for the nebula, based on either the mean values or our best measurement of a given line. The assumptions implicit in constructing this table are that neither the unresolved nebula nor the star is variable.

a) The Balmer Line Ratios

The nebular Balmer emission-line fluxes are difficult to measure, given the strong stellar absorption and blending problem. The very strong Hα line is affected only to a small extent. While we have analyzed primarily the absorption line wings in § III*a*, it is important to note that (1) the line cores are very sensitive to the surface gravity in the LTE models and (2) it is possible that the real stellar profiles show emission reversals, due to non–LTE effects or ongoing mass loss. Thus, the "basal flux" level of the stellar photosphere is uncertain, and the derived Balmer line ratios (as well as He II and He I lines) depend on what is assumed for the star. A further problem is that Hα and Hβ were not measured reliably with the same instrumentation.

Nonetheless, it is possible to judge at least qualitatively the behavior of the Balmer decrement by relying upon the adopted

flux values in Table 2C. This table uses the CCD spectra for Hα, assuming negligible stellar contamination, while using the high-resolution PCR data to isolate most of the line emission from Hβ and the higher Balmer lines. Since the stellar absorption decrement is steep, it is arguable that the contamination should decrease with increasing quantum number. Thus the ratio Hα/Hβ should be an upper limit, Hβ/Hγ a lower limit, and so on. The former ratio is 2.7, very close to the expected recombinational value in the low-density limit with negligible reddening. So is the latter value of 2.1. Thus, as far as can be determined, the Balmer decrement appears to be normal. This result also indicates that the Hβ flux utilized in § IV*d* is not a substantial underestimate.

b) Nebular Density and Temperature

The nebular spectrum is characterized by both forbidden and permitted lines. However, a first clue to the unusual physical conditions existing in this gas is evident from considering the "oxygen-temperature" ratio of the fluxes of

$$R([\text{O III}]) = [f(5007\ \text{Å}) + f(4959\ \text{Å})]/f(4363\ \text{Å}) \quad (2)$$

(see Table 2C). At the densities typical of planetary nebulae, R([O III]) is an estimator of the temperature of the ionized gas, at least for the region in which the [O III] exists. From Table 2C, we determine that R([O III]) for the compact nebula is only 12.9, while typical nebular values are as much as an order of magnitude greater. If the electron density (N_e) of the nebula were in the typical range of 10^2–10^4 cm^{-3}, this value would lead to an impossibly high estimate for the electron temperature (T_e), >50,000 K (see, for example, Osterbrock 1974, eq. [5.4], p. 100).

Such a high electron temperature would be unprecedented for a planetary nebula. All objects tabulated by Pottasch (1984, his Appendix I) have derived [O III] T_e within the range 8000–23,000 K. The cooling transitions such as those of [O III] are very effective thermostats under a wide variety of conditions. The electron temperature may be higher than average if the central star is extremely hot. Even in nebulae associated with stars with $T_{\rm eff} > 100{,}000$ K, however, the derived nebular T_e values remain near 20,000 K (Kaler 1983). Moreover, the results of § III*a* show that while the star's photosphere is hot, it is well below 100,000 K and far from extreme among known planetary nuclei. In addition, the emission-line spectrum does not indicate a nebula of very high excitation: the ratio of the permitted He II/Hβ lines is barely greater than zero, and the [Ne V] λ3425/[Ne III] λ3869 ratio is near zero. A second means by which the electron temperature may be increased is if the coolant gas has a low heavy-element abundance. Again, however, the derived values for the few known planetary nebulae in the halo of the Galaxy and for those in metal-poor extragalactic populations such as the Magellanic Clouds seldom exceed 20,000 K. For this object, anyway, the abundance estimates derived for the detected heavy elements are not too different from Population I (§ IV*g*). We can safely conclude that the T_e value implied by the [O III] ratio in the low-density limit is not plausible.

The [O III] line ratios are dependent solely on collisional excitation and T_e only if the electron density is low enough that collisional de-excitation cannot compete with the (rather long) time scale for radiative decay of the forbidden transitions. If N_e approaches 10^6 cm^{-3}, on the other hand, collisions may alter significantly the level populations relevant to these [O III] lines. At a given temperature, increased densities result in depopulation of the $^1D_2$ levels, which are the upper levels for the 4959 and 5007 Å emission lines, while the $^1S_0$ level from which the 4363 Å line occurs is less affected. At densities near 10^6, the longer wavelength [O III] lines begin to be "quenched," as do other forbidden lines at densities above their critical values. The value expected for the ratio of the [O III] lines then becomes a more complicated function of N_e and T_e which must be calculated using a model that includes both collisional and radiative processes in detailed balance.

Ionized gas at such high densities may occur in the line-emitting regions around active galactic nuclei and radio galaxies. In this context, the critical densities at which quenching of various forbidden lines occurs are listed in Filippenko (1985, Table 2C). For example, the critical N_e for the [O III] λλ4959 and 5007 transitions is 7.9×10^5, while that for [O III] λ4363 is much higher at 3.0×10^7. We are also fortunate that considerable modeling calculations performed to fit the observed emission lines of narrow-line regions in active galaxies are applicable to the physical conditions for this object. Predictions for the [O III] transitions appear in Figure 11 of Filippenko and Halpern (1984), which we shall use to estimate upper and lower density bounds: If it is assumed that the electron temperature T_e falls within the range referenced above (8000–23,000 K), then the observed value of R constrains the value of N_e to lie between 10^7 cm^{-3} (for the low T_e limit) and 4×10^5 (for the high end).

Comparison of fluxes for the remaining line spectrum with other entries in the Filippenko (1985) table leads to a picture generally consistent with the hypothesis that the nebular density lies within this range. [Ne III] λ3869, which is one of the strongest observed spectral lines, is quenched only at the high value of 1.2×10^7. On the other hand, such common nebular forbidden lines as the [O II] 3727 Å, [S II] 6716, 6731 Å, and [N II] 6583 Å doublets are quenched at densities below 10^5 cm^{-3} and are not detected in this line spectrum.

It is clear that the weak He II and other indicators point to only a moderate level of nebular excitation, so that at least some emission from the singly ionized doublets would normally be expected. The clinching argument, then, is the observation of low-excitation transitions which are quenched only at higher densities: First, the [O II] 7325 Å line, normally much weaker than the 3727 Å doublet in gaseous nebulae, is probably detected. This transition has a critical density of 5.9×10^6 cm^{-3}. Likewise, [O I] λ6300, quenched at 1.4×10^6 cm^{-3}, appears weakly, although this feature may be a blend with [S III] λ6312. This feature, detected in both observations on different nights, cannot be attributed to atmospheric auroral glow, since this would have been evident in the strengths of these lines in the sky spectra of these and other exposures. Another similar line, however, that is not detected is [S II] λ4069, which is quenched at a much lower value of 1.7×10^6 cm^{-3}. Generally, the forbidden-line spectrum appears to be consistent with the broad density range estimated above from the [O III] line ratio. It is difficult without a much more detailed model to pin down the T_e and N_e values more accurately.

c) Unresolved Nebular Core Component

In Figure 8 we display intensity profiles of the CCD spectrum perpendicular to the dispersion direction across (1) the [O III] 5007 Å and (2) an adjoining continuum interval. The profiles are virtually identical. The measured full width at half-maximum for each is approximately 3.0 pixels, consistent with

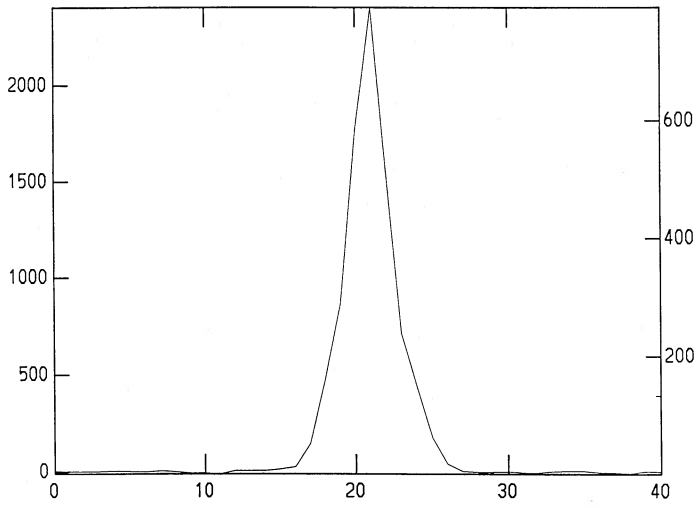

FIG. 8a

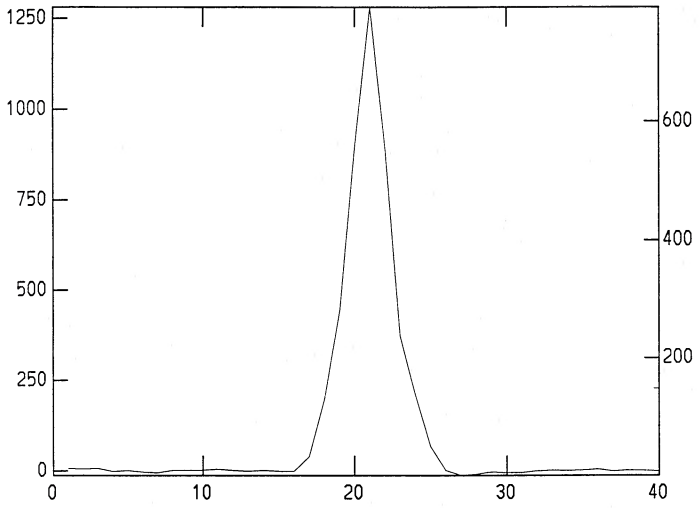

FIG. 8b

FIG. 8.—Two dimensional traces perpendicular to the direction of dispersion for the 4 m CCD spectrum from Fig. 3, in spectral bandpasses including (*a*) the 5007 Å emission line and (*b*) a region of only stellar continuum near 5100 Å.

a seeing diameter of 2".5. At the derived distance of 460(+174, −126) pc, the upper limit to the size of the [O III] emitting nebula is 1150 ± 350 AU. This turns out to be much larger than the ionization bound on the nebular size as discussed below.

d) Mass and Size of the Compact Nebula

Let us assume a simplified model of a fully ionized nebula at a single density and adopt a slightly enriched helium abundance of 40% by weight (see § IV*g*) but neglecting the heavier elements. We can estimate the nebular mass, despite the lack of a resolved nebular size, as

$$M_{\rm neb} = 11.06 F_{\rm H\beta}\, d^2 t^{0.88} N_e^{-1} \qquad (3)$$

(Pottasch 1984, p. 111) where $F_{\rm H\beta}$ is the flux measured at Earth (Table 1) in units of 10^{-11} ergs cm^{-2} s^{-1}, d is the distance in kpc, t is the electron temperature divided by 10,000 K, and $M_{\rm neb}$ is given in solar masses.

Using the values $F_{\rm H\beta} = 2.9 \times 10^{-14}/10^{-11} = 0.0029$ and $d = 0.460(+0.174, -0.126)$ kpc, the nebular mass is only

$$\begin{aligned} M_{\rm neb}/M_\odot &= 0.0069(d/0.460)^2 t^{0.88}/N_e \\ &= 3.6 \times 10^{-8}(d/0.460)^2 , \\ &\qquad N_e = 4 \times 10^5,\ T_e = 23{,}000\ {\rm K} , \qquad (4) \\ &= 5.7 \times 10^{-10}(d/0.460)^2 , \\ &\qquad N_e = 10^7,\ T_e = 8000\ {\rm K} . \end{aligned}$$

If the distance lies at the upper end of the range derived previously, the above numbers should be increased by approximately 100%; alternatively, at the low end of the distance range, they should be decreased nearly 50%. Thus, the ionized gas in the compact nebula should lie in the range 3×10^{-10} to $7 \times 10^{-8}\, M/M_\odot$.

This relatively small mass corresponds to a nebula of quite small physical extent, even if either the filling factor of the nebular volume or the covering fraction for intercepting the stellar radiation are much less than unity. For a spherically symmetric nebula of radius R, uniform density, and filling factor f,

$$M_{\rm neb} = (4\pi/3) N_e\, 1.4 m_{\rm H}\, f R_{\rm neb}^3 . \qquad (5)$$

The nebula might have a low filling factor if it were ejected as a discrete event (§ V*a*) and was now an expanding shell. Alternatively, f could be the fraction of 4π steradians over which optically thick gas intercepts the stellar radiation. Inverting the equation, we find that

$$R_{\rm neb} = 8(M/10^{-8}\ M_\odot)^{1/3}(N_e/10^6\ {\rm cm}^{-3})^{-1/3} f^{-1/3}\ {\rm AU}! \qquad (6)$$

Even for the most massive, lowest density extreme from equation (4), the radius is scarcely a factor of 2 larger (17 AU). In the high-density limit, it can be as small as 1.4 AU. If the filling factor or covering factor is less than unity, the linear extent of the nebula could of course be larger, but only as the $-\frac{1}{3}$ power.

Thus, the order of magnitude of the size of the ionized gas region established by the ionization bound—by the modest luminosities of the line-emitting region and white dwarf central star—is likely to be correct. The ionized region is no larger than our solar system! Ten astronomical units corresponds to only 0".02 at a distance of 460 pc, far smaller than the seeing-limited size of the nebula found in the previous section.

e) Radial Velocity, Expansion Rate, and Time Scale of the Compact Nebula

The two MMT echelle spectra (§ II), centered on the Hα and He II 4686 Å emission lines, were used to determine the radial velocity of the object. Gaussian profile fits to the strong Hα and weaker He II lines yielded heliocentric radial velocity measurements of $+6.2 \pm 1.8$ and $+19.2 \pm 9.4$ km s^{-1}, respectively. These consistent results support the assignment of the star to the disk population.

In the limit of low optical depth, the emission-line widths are a measure of the expansion velocities. For the strong Hα line, the full base width is about 140 km s^{-1}. For the weaker He II line, we measure 100 km s^{-1}. We suspect that the width of the former may be enhanced by optical depth effects in the Balmer lines, since the nebula is quite dense. If we can assume that the weak He II 4686 Å line is optically thin, and that it originates within the nebula and not within the stellar photosphere, then the derived expansion velocity of the compact nebula is not too different from 50 km s^{-1}. If there is significant line broadening due to optical depth effects or the contribution of a stellar photospheric component, this value may still be used as an

upper limit. The absence of broad wings appropriate to the stellar escape velocity indicates that there is little contribution to the total emission measure by material still near the surface of the white dwarf.

The size of the ionized gas region was found to be of order 10 AU (1.5×10^9 km) in § IV*d*. The time scale for ejected mass to escape from the ionization-bounded region is thus on the order of a year!

At the derived distance of 460 pc, the large, outer nebular shell of EGB 6 has a radius of 0.8 pc. Unfortunately, no quantitative measurements of the outer nebula are available. Assuming a 20 or 50 km s^{-1} average expansion velocity, the age of the extended component is 50,000 and 20,000 yr, respectively. This range is smaller by an order of magnitude than the cooling age of the white dwarf (several times 10^5 yr) estimated by comparing the derived stellar parameters with the predictions of evolutionary tracks. The implication is that even the outer nebular shell was ejected after the PNN had entered the white dwarf sequence far from the asymptotic giant branch (AGB). It is worth noting, however, that the same argument might be made for the extended nebula of Abell 7, since that nucleus has been assigned similar atmospheric parameters (Mendez *et al.* 1981). Thus, considerable reservation about this particular conclusion seems warranted.

f) Lack of Evidence for Variability of the Nebula

Given the unusually small indicated size and expansion time scale of the nebula, it is extremely interesting to scrutinize the various measurements of the line strengths recorded in Tables 2A and 2B. Recall that the use of equivalent widths is the best approach if the stellar energy distribution can be assumed to be constant. The independently determined (though uncertain) absolute line fluxes for the strong lines in Table 2B provide a means of examining for gross nebular variations, independent of this assumption about the central star. The possibility that the star could have varied drastically in the past is discussed in § V.

In fact, the comparison of the equivalent widths in Table 2A shows remarkable agreement among all observations! Moreover, there is no variation evident in Table 2B that we regard as significant. Recall that the PCR fluxes (last column) were obtained through the smallest entrance aperture, and are most likely to incur light losses. We conclude that there is no evidence for significant changes between 1978 and 1985–1987 in either the permitted- or the forbidden-line strengths, including those among the latter both sensitive and insensitive to density changes. However, we should caution that the inhomogeneity of the data set and relatively poor absolute spectrophotometry also make it difficult to conclude with confidence that the nebula has not varied somewhat. It would be worthwhile to measure the nebular fluxes on a continuing basis.

g) Abundances of the Nebula

The relative fluxes listed in Table 2C can be used to determine nebular abundances. A single choice of T_e and N_e within the estimated ranges was adopted for this purpose. For the former, 12,000 K is assumed, a not atypical value for nebulae showing stronger He I than He II lines; the electron density N_e is assumed to be 2.7×10^6 cm^{-3}, a value which is close to the geometric mean for the range given in § IV. The choice is consistent with the model of Filippenko and Halpern (1984) in producing the correct, observed [O III] line ratio. We utilized a program kindly provided by G. Jacoby, with standard relations for correcting the observed [O III], [Ne III], and helium lines for unseen ions. Argon abundances are not calculated, since the observed lines are weak and/or blended with other transitions. This standard program does not take into account the weakening of the oxygen line strengths due to quenching.

The calculated helium abundance number fraction is 0.13, some 40% higher than the solar fraction. This number is based on observed He I and He II line fluxes, without any correction for undetectable neutral helium. It is also possible that the derived helium abundance may be too high owing to neglect of collisional excitation in this dense nebula. The number abundances of oxygen and neon were calculated from only one observed ionization state each on the standard logarithmic scale with hydrogen equal to 12.00. The derived values of 8.6 for oxygen and 8.0 for neon are remarkably close to the mean for the sample of Galactic disk planetary nebulae analyzed by Aller and Czyzak (1983). However, the former might be treated as a lower limit, since quenching effects weaken the [O III] lines. The neon abundance should be more accurate, since [Ne III] is likely to be the dominant ionization state for a nebula of this excitation, and the observed line is not subject to quenching. It is usually argued that the neon and oxygen abundances are not substantially changed by prior nucleosynthesis and mixing processes of the progenitor star; on the other hand, it is found that the PN helium abundance may often be significantly larger than the initial value assignable to the progenitor population.

These results represent only a cursory analysis of a complicated nebula, but they provide no surprises and are consistent with assigning this object to the Galactic disk population. They indicate that the recent ejecta from the star have a predominantly hydrogen-rich composition, with no strong indication of either enrichment or depletion of heavy elements. We note that it was not possible to determine from the spectra of the white dwarf whether the photospheric abundances of helium and heavy elements are similar.

V. DISCUSSION

The results of §§ III and IV may be summarized as follows: A dense nebula exists around the white dwarf nucleus, with an ionized mass ranging from a few times 10^{-10} to several times 10^{-8} $M_\odot$. Given the modest luminosity of the 70,000 K DA white dwarf, the Lyman-continuum photons are all absorbed within a distance of order 10 AU or less. For a filling factor or covering factor (f) much less than unity, this scale increases only as $f^{1/3}$. At the indicated expansion rate of $\lesssim 50$ km s^{-1}, any parcel of nebular matter passes out of the ionized region in a time on the order of 1 year or less. Thus, if the gas were being ejected in a steady process, the mass-loss rate per year should be close to the range of masses given above. The line fluxes in the outer nebular rim component of EGB 6 may provide a useful diagnostic for the geometry of the inner nebula. The large shell presumably emits a smaller integrated line flux, but that may require a nonnegligible fraction of the ionizing flux of the central star. In that case, the spherical symmetry of the outer rim combined with the success of the ionization-bounded model would suggest a non–spherically symmetric (disklike) or patchy inner nebula.

The nebular mass and radius estimated for the inner, unresolved region are tiny in comparison with those normally measured for planetary nebulae, but it is clear that these small

values may simply be a consequence of the modest stellar luminosity. It is therefore somewhat misleading to make comparisons with the properties of nebulae which generally represent the initial ejections by luminous stars leaving the top of the AGB in the H-R diagram (having nebular masses of order 0.01–1 $M_\odot$). Nonetheless, it is worth noting that the nebular mass decreases with increasing N_e for normal planetaries (cf. Pottasch 1984, Fig. V-9). The densest nebulae are associated with the youngest PNNs nearest the AGB, and the nebular expansion velocity measured for this compact nebula is also quite similar to those of young planetaries!

We consider three kinds of hypotheses to account for the recent mass loss associated with 0950+139. First, we explore the possibilities that the mass was ejected as a discrete event, such as a thermal pulse or nuclear-burning instability of the central star. This scenario must reconcile some severe time scale constraints, as discussed below. Second, we consider the possibility that the mass loss from the white dwarf is an ongoing event; for this there appears to be no theoretically established mechanism to explore. Third, the possibility that the object is some kind of close binary system is discussed. A detailed photoionization model for the compact nebula is presented in a second paper by Dopita and Liebert (1989); this leads to a consideration of a different scenario for the origin of the gas.

a) A Discrete Ejection Event?

Both helium and hydrogen shell source instabilities have been proposed for degenerate stars of $\log(L/L_\odot) \sim 1$ or fainter. In each case, the calculations require the star to expand in size and visit a region of high luminosity in the H-R diagram at least briefly. This allows any ejected matter to escape while the star has temporarily a much larger radius, so that the observed nebular velocities are therefore of the same order of magnitude as the escape velocity of a red giant. The star must return to its original size and luminosity fast enough to be found still embedded in a nebula of density of order 10^6 cm^{-3} or higher. The compact nebula should dissipate or change radically in density within a few years (or less) unless one contrives a special geometry. For the last 10 years of spectrophotometric and photometric observations, the star has apparently been a 16th magnitude white dwarf with no apparent light variability (see § IIc). It appears to be of similar magnitude and very blue color on the Palomar Observatory Sky Survey prints, images dating from 1954 February. From this we can conclude that any secular decline in brightness from a nova-like event must have ended more than 30 years ago; this is a conservative lower limit to the time of principal mass ejection in this kind of model. It poses a very severe constraint indeed!

The helium shell flash (cf. Schönberner 1979; Iben *et al.* 1983) appears to face a severe mismatch in time scales, since models predict a long phase ($>10^4$ yr) of quiescent helium burning at high luminosity before it returns to its initial luminosity (see Iben *et al.* 1983, Fig. 1). The flash is comparatively deep in the stellar envelope, since the mass above the helium shell source is believed to be of order 10^{-2} $M_\odot$. A second pitfall is that the flash would likely eject the outer hydrogen layer, which has 2 orders of magnitude less mass, resulting in a helium- and probably carbon- and oxygen-enriched stellar surface (possibly affecting the nebula as well). The unusual planetary nebulae Abell 30 and Abell 78 have inner nebular knots which are quite hydrogen-deficient and encompass hydrogen-deficient central stars (Jacoby and Ford 1983; Kaler 1983). It has been proposed (Iben *et al.* 1983) that these objects have recently undergone helium shell events.

Perhaps an even more appropriate comparison is with the case of the unusual nova V605 Aql. During an apparent outburst event, this object reached apparent magnitude 10 in 1919 and remained bright for several years, but has been below 20th magnitude in recent decades (Bidelman 1971). Its spectrum at maximum light was that of a hydrogen-deficient carbon red giant (Bidelman 1973). V605 Aql is also the central star of the low surface brightness planetary nebula Abell 58 (van den Bergh 1971), whose slow expansion rate (Ford 1971) shows that it was ejected long before the 1919 outburst. A compact, unresolved emission nebulosity was discovered by H. E. Bond and P. Osmer (1988, private communication) and, independently, by Seitter (1985). The compact nebula is extremely hydrogen-deficient, showing only emission lines of [O III] and [N II] (Seitter 1985, 1987). Following Pottasch (1985) and Seitter (1987), we suggest that V605 Aql has undergone a helium shell runaway event, although the observed time scale for fading is orders of magnitude faster than the predictions of Iben *et al.* (1983). The rapid time scale might be possible if so much of the helium envelope were ejected that it could not sustain the helium shell burning, and/or if the stellar mass were unusually high (~ 1 $M_\odot$). In any event, V605 Aql may provide rather direct observational evidence for the temporary transformation of a planetary nucleus into a red giant, with accompanying mass loss. However, like the nuclei of Abell 30 and Abell 78, V605 Aql is likely to evolve (or may already have evolved) into a non-DA white dwarf, while 0950+139 has remained a hydrogen-rich DA white dwarf.

A hydrogen shell flash or "self-induced nova" (Iben and MacDonald 1986) has fewer drawbacks as an explanation for a discrete event in 0950+139. Since only the hydrogen layer is involved, it is not necessary to assume that all of the hydrogen would be lost or that the nebula or stellar surface would be enriched in helium. Moreover, the amount of mass external to the hydrogen shell source is only of order 10^{-4} $M_\odot$. Hence, it is plausible to assume that the star may return more quickly from the red giant region to essentially its starting point on the white dwarf sequence. However, the calculations of Iben and MacDonald (see their Fig. 12) were ended some 9 years after the shell flash, with the star at $\log(L/L_\odot) > 4$. If there is no significant heating of deeper layers, it is plausible to assume that the star might take a comparable time—of order 10 years—to return to the vicinity of its starting point (see also Iben 1982). If we were then to hypothesize that the mass ejection covers a relatively small solid angle—perhaps an outflow in the form of collimated "jets"—then the size constraint is relaxed and the expansion velocity might translate into a dissipation time scale of the order of tens of years.

This argument appears contrived, however. The derived size of the region of ionized gas increases only as the filling factor to the $-\frac{1}{3}$ power. The outer nebular rim is much too large to be associated with any recent nova-like event, but Iben and MacDonald argue that the hydrogen shell instability may recur often, and might eventually result in the stripping away of the entire hydrogen layer. More theoretical calculations appear necessary in order to assess whether this scenario can really satisfy the time scale constraints outlined above.

The absence of evidence for variability of the [O III] 5007 Å line and of other density-sensitive transitions also may be inconsistent with a discrete-event hypothesis. If the ejected nebula were expanding as a shell at constant velocity, the

density should be decreasing with shell radius (r) and time since the ejection (t) as

$$N_e \propto r^{-2} \propto t^{-2} . \quad (7)$$

However, the detectability of this change depends on how long ago one hypothesizes the event to have occurred. The observations of the star appear to require that such an event happened before about 1950. For example, if the eruption took place 50 years ago, the shell size might now be of the order of hundreds of astronomical units, and the density might have decreased only by about 40% in the last 10 years. We doubt that the observations assessed in § IV*f* are accurate enough to rule out a decrease of this amount.

b) A Steady Wind?

If the mass loss is characterized as an ongoing wind of unknown origin, a mass-loss rate of the order of a few times 10^{-10} to several times 10^{-8} $M_\odot$ yr^{-1} is inferred from the nebular velocity and radius and the range of estimates for the ionized mass. Not only has no plausible mechanism for this amount of mass loss from a white dwarf been proposed, but there is little observational evidence for extensive mass loss from any known star of comparable surface gravity. A few DA white dwarfs may show evidence for selective winds of radiatively driven ions (Bruhweiler and Kondo 1983). A few hot degenerates show weak emission lines (Sion, Liebert, and Wesemael 1985; Reid and Wegner 1988), but these appear to occur at the top of the atmosphere rather than in a circumstellar H II region.

A severe difficulty for the hypothesis is the need to explain how the apparent expansion velocity is some 2 orders of magnitude lower than the escape velocity of the host star, thus seeming to require a "fine tuning" of the mass-loss mechanism. As noted previously, the Hα and He II 4686 Å emission lines (Fig. 5) lack the broad wings expected if there were a significant contribution to the line flux from matter near the star. Since the cause is unspecified, however, it is difficult to explore this possibility further, although in § V*d* we consider some possible consequences.

c) A Close Binary System?

One way of solving the escape velocity problem mentioned in the previous section would be to place the launch point for the material away from the surface of the white dwarf. Note that the emission measure requires a nebula orders of magnitude larger than a plausible companion's magnetosphere or envelope. We can hypothesize that 0950+139 is a close, detached binary in which enhanced mass loss from a low-luminosity companion might be induced by the strong far/extreme ultraviolet flux of the close primary star.

The facing side of the secondary will be heated to a temperature T_2 as a result of reprocessing of radiation from a hot star of temperature T_1 and radius R_1 at a separation a given by

$$(T_2/T_1)^4 = 0.5(R_1/a)^2 , \quad (8)$$

where the units of distance are $R_\odot$. For the derived parameters of 0950+139 this predicts that significant excess optical radiation would be observed ($T_2 \gtrsim 5000$ K) if $a \lesssim 3$ $R_\odot$, corresponding to an orbital period $\lesssim 1$ day. This excess radiation should modulate with the orbital period unless the binary is viewed pole-on. Yet even with that unfavorable geometry, excess radiation from half of the observed secondary's cross section would produce an excess at longer wavelengths in the energy distribution over the observed Rayleigh-Jeans–like slope (Fig. 4). Dramatic examples of these effects include BE UMa (Ferguson *et al.* 1987) and some binary planetary nebula nuclei discovered by Bond and Grauer (1987). The former consist of an 80,000 K white dwarf and an M dwarf in a system with a period near 2 days. However, the known close, detached pairs involving hot white dwarfs do not show evidence for substantial mass loss from the secondary star, nor do any show a nebula similar to that observed with 0950+139. V471 Tauri is a special case: the K dwarf companion shows activity not unlike the RS CVn variables, including an extremely active wind. As is typical of late-type dwarfs with active chromospheres, however, the wind is very fast. The outflow velocities of thousands of kilometers per second (Sion, Bruhweiler, and Mullan 1988) are orders of magnitude higher than those possible for the compact nebula in 0950+139.

Although the available information is insufficient to rule out the existence of a close binary in 0950+139, it is difficult to imagine how such a companion could be contributing to the production of the nebula without being detectable in one of the ways discussed above and in § II*c*.

d) Possible Implications for White Dwarf Evolution

Regardless of whether the cause is discrete or steady in nature, let us consider the possibility that the mass-loss phenomenon observed in this DA white dwarf at the high-luminosity end of the sequence is relevant in a general sense to the evolution of these objects. It is even possible that the study of this object can help explain an apparent dilemma in reconciling contrasting conclusions concerning the thickness of outer hydrogen envelopes in H-rich PNNs and DA white dwarfs (Liebert 1989). In particular, Schönberner (1981, 1986, 1987) argues that the majority of planetary nuclei must be hydrogen shell burning objects, requiring the outer hydrogen layers to be "thick" ($\sim 10^{-4}$ $M_\odot$). This conclusion is in apparent conflict with a variety of evidence based on studies of the white dwarfs at various temperatures, indicating that the DA white dwarfs have outer hydrogen layers many orders of magnitude thinner than 10^{-4} $M_\odot$ (Fontaine and Wesemael 1987).

The possible clue offered by the case of 0950+139 is that the thinning of the outer hydrogen envelope may occur very late in the evolution of the planetary nuclei with hydrogen-dominated atmospheres and may extend into the hot white dwarf region. If the mass loss is assumed to occur during the PNN stage for the typical 0.6 $M_\odot$ object, this requires that of the order of 10^{-4} $M_\odot$ of hydrogen envelope be lost in a few times 10^4 yr, or an average rate of order 10^{-8} $M_\odot$ yr^{-1}. This value appears to be higher than any values derived for PNNs with H-rich atmospheres (cf. Vauclair and Liebert 1987).

The required average mass-loss rate is much lower if we can assume that the material is lost after the star has entered the slower evolutionary phase of white dwarf cooling. There is evidence for selective mass loss in hot DA white dwarfs (Bruhweiler and Kondo 1983); however, the outflow occurs in a few known stars only in selective, radiatively driven lines. While we have not been able to find any estimates of mass-loss rates associated with this phenomenon, there is no evidence that such stars possess a general wind of order 10^{-10} $M_\odot$, which is the required average rate over the cooling age of a very hot white dwarf ($\lesssim 10^6$ yr).

The steep luminosity function of white dwarfs now becomes a severe impediment to the testing of how general this phenom-

enon of associated emission nebulosity might be. We have searched too small a volume of space to test whether DA white dwarfs with $T_{\rm eff} \geq 70{,}000$ K generally go through such a phase! In the carefully observed sample of Holberg *et al.* (1989), there is one other case which has a similar temperature; the rest are cooler. The planetary nuclei of Abell 7 and NGC 7293 also have $T_{\rm eff} \geq 70{,}000$ K and surface gravities similar to those of the nebula-free white dwarfs. Their optical and ultraviolet spectra show no superposed emission lines and hence no evidence for a similar, compact nebula (Mendez, Kudritzki, and Simon 1983; Heap 1983; Wesemael, Green, and Liebert 1985).

The available null results from a dozen or so well-studied white dwarfs at 50,000–60,000 K (Holberg, Wesemael, and Basile 1986; Fleming, Liebert, and Green 1986; Holberg *et al.* 1989) indicate that the frequency of such "mini–planetary nuclei" events is also low for somewhat cooler stars.

e) Some Follow-up Work

This "discovery paper" ends without a clearly successful hypothesis as to either the origin of the compact nebula observed uniquely in this hot dwarf or how its existence might relate to some general problems in the evolution of hot, post–AGB stars. Further study is clearly warranted on several fronts. A detailed photoionization model of the nebula leads to improved nebular parameters (Dopita and Liebert 1989). Further theoretical studies of late thermal pulses in hydrogen and helium thin shell sources would clarify the expected time scale for variability. Continued spectroscopic measurements of the line fluxes of the unresolved nebular component should focus on detecting changes in the density-sensitive forbidden lines. Note that as long as the filling/covering factor does not change, any increase or decrease in an ongoing mass-loss rate would not result in any significant change in the luminosities of permitted lines and density-insensitive forbidden lines. A modulation in the mass-loss rate would result in a change in the radius and mean density of the ionization-bounded region. If the mass loss were a discrete event, the density should be decreasing with time.

Sensitive mapping of the ionized gas at higher spatial resolution with the HST might have a chance of resolving the central component. Wide-field imagery could more accurately determine the distribution and measure the flux of the extended nebular component, thus exploring for "leaks" in the ionization bound of the recently ejected gas. If velocity mapping were possible, the results might determine the time scale over which mass loss has occurred, owing to either discrete or continuous events. A search of archival plates for variability of the central star would be an important test for a discrete-event hypothesis.

A careful search for nebulosity around the known, hottest DA and DO white dwarfs at various spatial scales might help place 0950+139 in a better general context. Reid and Wegner (1988) show convincingly that the weak Hα emission component observed in G191-B2B is not due to circumstellar gas. Moreover, it is necessary to expand the known sample of very hot DA stars. While some of this can be accomplished by optical surveys, we note that such future space-based surveys as the *EUV Explorer* satellite and *ROSAT* are anticipated to have a large yield of such stars (cf. Finley, Malina, and Bowyer 1987; Barstow 1989).

We acknowledge useful conversations with Lawrence Aller, Todd Boroson, Alex Filippenko, Jesse Greenstein, Manuel Peimbert, Alvio Renzini, Hugh Van Horn, and Ray Weymann. We thank the anonymous referee for several criticisms which improved the paper. This work was supported by the National Science Foundation through grant AST 88-40482 (J. L.), by NASA through grant NAG 5-434 (J. H.), and by the NSERC Canada.

REFERENCES

Aller, L. H., and Czyzak, S. J. 1983, *Ap. J. Suppl.*, **51**, 211.
Barstow, M. 1989, in *IAU Colloquium 114, White Dwarfs*, ed. G. Wegner (Berlin: Springer), p. 156.
Bidelman, W. P. 1971, *Ap. J. (Letters)*, **165**, L7.
———, 1973, *Bull. AAS*, **5**, 442.
Bond, H. E., and Grauer, A. D. 1987, in *IAU Colloquium 95, The Second Conference on Faint Blue Stars*, ed. A. G. Davis Philip, D. S. Hayes, and J. Liebert (Schenectady: Davis), p. 221.
Bruhweiler, F. C., and Kondo, Y. 1983, *Ap. J.*, **269**, 657.
Dopita, M. A., and Liebert, J. 1989, *Ap. J.*, in press.
Ellis, G. L., Grayson, E. T., and Bond, H. E. 1984, *Pub. A.S.P.*, **96**, 283 (EGB).
Ferguson, D. H., Liebert, J., Cutri, R., Green, R. F., Willner, S. P., Steiner, J. E., and Tokarz, S. 1987, *Ap. J.*, **316**, 399.
Filippenko, A. V. 1985, *Ap. J.*, **289**, 475.
Filippenko, A. V., and Halpern, J. H. 1984, *Ap. J.*, **285**, 458.
Finley, D. S., Malina, R. F., and Bowyer, S. 1987, in *IAU Colloquium 95, The Second Conference on Faint Blue Stars*, ed. A. G. Davis Philip, D. S. Hayes, and J. Liebert (Schenectady: Davis), p. 689.
Fleming, T. A., Liebert, J., and Green, R. F. 1986, *Ap. J.*, **308**, 176.
Fontaine, G., and Wesemael, F. 1987, in *IAU Colloquium 95, The Second Conference on Faint Blue Stars*, ed. A. G. Davis Philip, D. S. Hayes, and J. Liebert (Schenectady: Davis), p. 319.
Ford, H. C. 1971, *Ap. J.*, **170**, 547.
Green, R. F., Schmidt, M., and Liebert, J. 1986, *Ap. J. Suppl.*, **61**, 305.
Heap, S. R. 1983, in *IAU Symposium 103, Planetary Nebulae*, ed. D. R. Flower (Dordrecht: Reidel), p. 375.
Heiles, C. 1975, *Astr. Ap. Suppl.*, **20**, 37.
Holberg, J. B. 1987, in *IAU Colloquium 95, The Second Conference on Faint Blue Stars*, ed. A. G. Davis Philip, D. S. Hayes, and J. Liebert (Schenectady: Davis), p. 285.
Holberg, J. B., Kidder, K., Liebert, J., and Wesemael, F. 1989, in *IAU Colloquium 114, White Dwarfs*, ed. G. Wegner (Berlin: Springer), p. 188.
Holberg, J. B., Wesemael, F., and Basile, J. 1986, *Ap. J.*, **306**, 629.
Iben, I., Jr. 1982, *Ap. J.*, **259**, 244.
Iben, I., Jr., Kaler, J. B., Truran, J. W., and Renzini, A. 1983, *Ap. J.*, **264**, 605.
Iben, I., Jr., and MacDonald, J. 1986, *Ap. J.*, **301**, 164.
Jacoby, G. H., and Ford, H. C. 1983, *Ap. J.*, **266**, 298.
Kaler, J. B. 1983, *Ap. J.*, **271**, 188.
Koester, D., and Schönberner, D. 1986, *Astr. Ap.*, **154**, 125 (KS).
Liebert, J. 1989, in *IAU Symposium 131, Planetary Nebulae*, ed. S. Torres-Peimbert (Dordrecht: Reidel), p. 545.
Mendez, R. H., Kudritzki, R. P., Gruschinkske, J., and Simon, K. 1981, *Astr. Ap.*, **101**, 323.
Mendez, R. H., Kudritzki, R. P., and Simon, K. P. 1983, in *IAU Symposium 103, Planetary Nebulae*, ed. D. R. Flower (Dordrecht: Reidel), p. 343.
Oke, J. B. 1974, *Ap. J. Suppl.*, **27**, 21.
Osterbrock, D. E. 1974, *Astrophysics of Gaseous Nebulae* (San Francisco: Freeman).
Paerels, F. 1987, Ph.D. thesis, Rijksuniversiteit Utrecht.
Petre, R., Shipman, H. L., and Canizares, C. 1986, *Ap. J.*, **304**, 356.
Pottasch, S. R. 1984, *Planetary Nebulae* (Dordrecht: Reidel).
———. 1985, in *Proc. ESO Workshop on Production and Distribution of* CNO *Elements*, ed. I. J. Danziger, F. Matteuchi, and K. Kjär (Garching: ESO), p. 258.
Reid, N., and Wegner, G. 1988, *Ap. J.*, **335**, 953.
Reynolds, R. J. 1987, *Ap. J.*, **315**, 234.
Schönberner, D. 1979, *Astr. Ap.*, **79**, 108.
———. 1981, *Astr. Ap.*, **103**, 119.
———. 1986, *Astr. Ap.*, **169**, 189.
———. 1987, in *IAU Colloquium 95, The Second Conference on Faint Blue Stars*, ed. A. G. D. Philip, D. S. Hayes, and J. Liebert (Schenectady: Davis), p. 201.
Seaton, M. J. 1979, *M.N.R.A.S.*, **187**, 73P.
Seitter, W. C. 1985, in *Proc. ESO Workshop on Production and Distribution of* CNO *Elements*, ed. I. J. Danziger, F. Matteuchi, and K. Kjär (Garching: ESO), p. 253.
———. 1987, *ESO Messenger*, No. 50, p. 14.
Sion, E. M., Bruhweiler, F. C., and Mullan, D. J. 1988, *Bull. AAS*, **20**, 706.

Sion, E. M., Liebert, J., and Wesemael, F. 1985, *Ap. J.*, **292**, 477.
Spitzer, L. 1978, *Physical Processes in the Interstellar Medium* (New York: Wiley).
van den Bergh, S. 1971, *Pub. A.S.P.*, **83**, 819.
Vauclair, G., and Liebert, J. 1987, in *Exploring the Universe with the IUE Satellite*, ed. Y. Kondo *et al.* (Dordrecht: Reidel), p. 355.
Vennes, S., Pelletier, C., Fontaine, G., and Wesemael, F. 1988, *Ap. J.*, **331**, 876.
Weidemann, V., and Koester, D. 1984, *Astr. Ap.*, **132**, 195.
Wesemael, F., Auer, L. H., Van Horn, H. M., and Savedoff, M. P. 1980, *Ap. J. Suppl.*, **43**, 159.
Wesemael, F., Green, R. F., and Liebert, J. 1985, *Ap. J. Suppl.*, **58**, 379.

HOWARD E. BOND: Space Telescope Science Institute, 3700 San Martin Drive, Baltimore, MD 21218

THOMAS A. FLEMING: Max-Planck-Institut für Extraterrestrische Physik, Karl-Schwarzschild-Strasse 1, D-8046 Garching bei München, Federal Republic of Germany

JAMES LIEBERT: Steward Observatory, University of Arizona, Tucson, AZ 85721

RICHARD F. GREEN: Kitt Peak National Observatory, National Optical Astronomy Observatories, 950 N. Cherry Street, P.O. Box 26732, Tucson, AZ 85726

JAY B. HOLBERG and KENNETH KIDDER: Lunar and Planetary Laboratory West, University of Arizona, Gould Simpson Building, 9th Floor, Tucson, AZ 85721

F. WESEMAEL: Département de Physique, Université de Montréal, C.P. 6128, Succ. A, Montreal, PQ, Canada H3C 3J7